ELSEVIER

Journal of Nuclear Materials 245 (1997) 248–252

journal of nuclear materials

Irradiation-driven solute redistribution in Zr alloys

H. Zou [a,*], G.M. Hood [a,1], J.A. Roy [a,2], R.H. Packwood [b]

[a] *AECL Research, Chalk River Laboratories, Chalk River, Ont., Canada K0J 1J0*
[b] *Metals Technology Laboratories, CANMET, Ottawa, Canada*

Received 2 July 1996; accepted 2 October 1996

Abstract

Zr–2.5Nb, with four different Fe concentrations, Zircaloy-2 and a Zr(Fe) single crystal have been irradiated with energetic Ar^+ ions (mostly 1.5 MeV) to fluences $\leq 10^{21}/m^2$ ($\sim$ 100 dpa). The resulting enhancement of the α-phase Fe solubility has been measured as a function of dose, dose-rate and specimen temperature. Most of the chemical analyses were done by electron microprobe. At 50 and 300°C there was a discernible increase in α-phase Fe for Zircaloy-2, but not for Zr–2.5Nb. Between 411 and 469°C the Fe levels in the α-phase of both alloys increased to $\sim$ 2500 ppma from prior-irradiation levels of $\sim$ 70 ppma: in Zr–2.5Nb thin foils there was a corresponding drop of the β-phase Fe concentrations from about 1.5 to 0.4 at.%.

1. Introduction

Many experimental investigations of the effect of neutron irradiation on phase stability and on the decomposition of Fe-bearing intermetallic precipitates in the Zircaloys and in Zr–2.5Nb (henceforth Zy and ZN, respectively) have been made in the past decade. It has been shown that irradiation causes Fe to be depleted from precipitates in Zy [1–4] and from the β-phase of ZN [5,6]. Recent work [7], using 1.5 MeV Ar^+ beams, has shown that much of the Fe transfers to the α-phase to form what appear to be radically-enhanced solid solutions (with respect to thermal equilibrium properties). The work of Ref. [7], published in 1995, was the first quantitative study of the effect of irradiation on the level and distribution of Fe in the bulk α-phase of Zy and ZN.

Under thermal equilibrium conditions, Fe in the α-phase of Zr, though only weakly soluble [8], controls self- and substitutional diffusion [9,10], with an implied influence on diffusional creep. Under irradiation conditions both creep and growth may be expected to be subject to the influence of Fe in the α-phase [11,12]. This is supported by recent work showing that in-service irradiation deformation of Zr–2.5Nb pressure tubes correlates with the Fe concentration of the alloys [12].

The present investigation extends the previous study [7] of Ar-irradiation-enhanced solubility of Fe in the α-phase of Zr alloys, to investigate that enhancement as a function of temperature, dose, dose-rate, and beam energy, as well as of the alloy Fe concentration. The first results are also reported for Kr irradiations and for Fe distributions in Ar irradiated α-Zr single crystals.

2. Experimental

2.1. Specimen preparation

In this study Zr single crystals containing $\sim$ 50 ppm Fe (all concentrations herein are in atomic units), Zy and four ZN alloys (ZN1-4) with different Fe concentrations, were irradiated. The composition of Zy is: Zr + 1.04% Sn, 0.56% O, 0.28% Fe, 0.23% Cr, 0.09% Ni; and of ZN, Zr + 2.5% Nb, 0.62% O and *X* Fe, where for ZN 1-4, *X* = 300, 900, 1340 and 2500 ppm, respectively. A special

* Corresponding author. Present address: Mat-Tech Co., 219 Bell Street North, Suite 908, Ottawa, Ont., Canada K1R 7E4. Tel.: +1-613 236 4909; fax: +1-613 236 7961; e-mail: henry@istar.ca.

[1] Retired.

[2] Retired.

PII S0022-3115(96)00711-8

Zr–2.5Nb alloy, ZNS, made from very-low Fe Zr (< 1.0 ppm) was also studied. The average grain size for Zy was 40 μm and for ZN 1-4, 9, 12.6, 3.5 and 11.1 μm, respectively.

The details of the alloy preparations are as described elsewhere [13]. Three types of specimen were used: bulk discs (3 mm diam × 0.1 mm), TEM foils and a bulk single crystal (6 mm diam × 2 mm thick). The disc specimens were prepared by mounting the discs in plastic resin and grinding them through successively finer SiC paper to 3 μm diamond paste. The final treatment was a chemical polish for 10 to 20 s in 50 H_2O:40 HNO_3:10 HF, by volume.

2.2. Irradiation conditions and analyses

The specimens were irradiated to fluences of ~ 0.05–1.0×10^{21} m^{-2} over periods of from 0.5–30 h, corresponding to an average damage of about 2–100 dpa through the penetrated depth. The two-directional sweeping system produced an overall homogeneity of better than ±5% for an irradiated area of 0.75 × 0.75 ($\times 10^{-4}$ m^2). The residual pressure adjacent to the specimens was $< 1 \times 10^{-6}$ Pa. Temperatures were measured with the aid of a thermocouple brazed to the specimen holder. Irradiations were carried out between 50 and 469°C for different sets of specimens; the beam was maintained during cooling down to ~ 100°C.

After irradiation, electron probe microanalysis (EPMA) was applied to determine the Fe levels in the irradiated volume (IRV) of the α-phase of Zy and ZNS — see Ref. [7]. Measurements (EPMA) of Fe in the α-phase of Zy and ZN were made at the centres of large α-grains, to avoid the effect of grain boundary precipitates. Typically 5–10 individual measurements were made on different grains. When small grains were examined, the beam was rastered to cover square patches, 2 to 5 μm on edge; for larger grains as many as ten closely adjacent readings were recorded. These strategies were employed to reduce residual carbon contamination of the analytical area to a minimum. Different beam energies were used to assess the depth distribution of Fe.

Secondary ion mass spectrometry (SIMS) was used to profile the Fe distributions of annealed reference and irradiated Zr single crystal specimens as functions of depth. Transmission electron microscopy (TEM) was used to examine the microstructural changes in irradiated foils and energy dispersive X-ray analysis (EDX) was used to measure the Fe levels in the β-phase of irradiated foils.

3. Results and discussion

The results of Fe measurements on irradiated alloys are presented in Tables 1 and 2. Table 1 presents the Fe levels in the IRV of the α-phase, measured by EMPA, and Table 2 presents the Fe levels in the β-phase of irradiated foils measured by EDX. The results in the tables are associated with an uncertainty of about 20% for > 100 ppm, and up to 50% for < 100 ppm. Unless specified otherwise, all the concentration data in the tables, and in the discussions hereafter, refer to α-phase measurements. The Fe levels in the unirradiated α-phase of ZN and Zy are generally expected to be about 70 ppm [13]. The Fe levels for ZNS after irradiation were found to be negligible, ruling out contributions from contamination or artefacts.

Table 1
Fe levels (ppm) in Ar irradiated Zr α-phase

Exp. [a]	Temp. (°C)	Time (s)	Dose (ions m^{-2})	ZN1	ZN2	ZN3	ZN4	Zy-2
1	ref.			67	58	48	175	70 [a]
2	303	7.2×10^4	7.38×10^{20}	181	107	–	893	1100
3a	420	1.73×10^4	1.96×10^{20}	414	576	1223	1801	
b				733	973	2260	2742	
4	411	3.67×10^4	3.96×10^{20}		769	1350		
						foil	1952	
5	446	6.94×10^4	7.94×10^{20}			1266		
6	480	7.2×10^3	1.11×10^{20}	329	825	1277	1139	
7a [b]	420	1.44×10^4	2.18×10^{20}	453	649	936	1832	
b				659	766	1333	2450	
8	420	1.8×10^3	4.12×10^{19}	217	118	828	671	
9	420	3.6×10^4	5.33×10^{19}	153	229	361		201
10a [c]	420	1.44×10^4	1.01×10^{20}	140	513	499	688	
b				135	645	583	1443	

The measurements labelled 'b' were made with a 10 kV electron probe beam, otherwise a 20 kV beam was used.
[a] Not measured here, see Section 3.
[b] The accelerating voltage here was 400 kV.
[c] The irradiation particle here was 1.5 MeV Kr.

Table 2
Fe levels in the β-phase of irradiated and unirradiated ZN foils

Specimen	Temp. (°C)	Time (s)	Dose (ions m^{-2})	Nb level (at.% [a])	Fe level (at.% [a])
ZN3	ref.			17.45	1.61
ZN3	446°C	19.3 h	7.94×10^{20}	18.43	0.65
ZN3	469°C	24.25 h	9.41×10^{20}	19.28	0.37

[a] These are the average of three measurements.

The individual irradiation experiments will be discussed in the order of their presentation in Table 1. Prior to that a general comment on irradiations with different nucleons/ions will be given.

3.1. Damage distribution

Compared with similarly energetic neutrons, protons and electrons, Ar^+ and Kr^+ have much higher displacement rates and much smaller ranges. This restricts the damage to relatively near-surface regions with a very high damage density. 'TRIM' calculations [14], see Fig. 1, show that for 1.5 MeV ions, the Ar and Kr profiles peak near 0.8 and 0.55 μm, respectively, tailing to more than 1 μm, and that the damage profiles peak near 0.6 and 0.35 μm, respectively, also tailing to around 1 μm. The damage peaks are shifted towards the surface with relative intensities ranging from 0.2:0.8 and 1.1:1.9, surface to peak, for Ar and Kr, respectively. The depths of interest

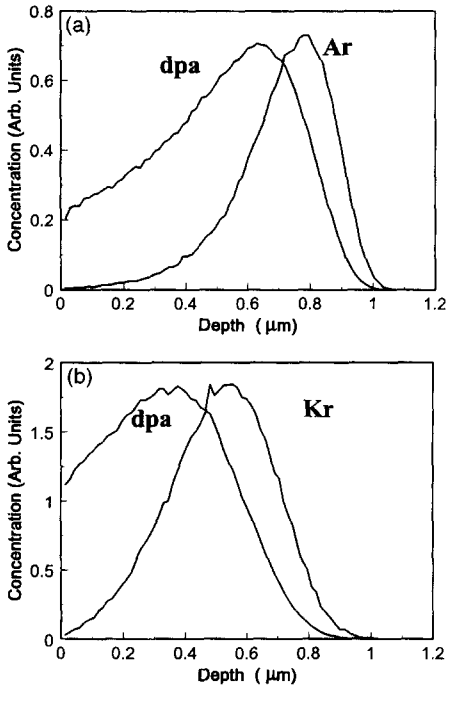

Fig. 1. Results of Trim calculations for ion ranges and damage distributions in Zr for (a) 1.5 MeV Ar^+ and (b) 1.5 MeV Kr^+.

are generally comparable with the EMPA probing depth, ~ 1 μm at 20 kV.

3.2. Zr alloys

Exp. 1. The α-phase Fe levels for the unirradiated specimens are about 60 ppm for ZN1-3 and 175 for ZN 4. The results for ZN1-3 and Zy are quite comparable to previous, equivalent, values [13].

Exp. 2. The longer irradiation time here, 20 h, versus 3 h in the previous parallel investigation [7], has led to a relatively higher (3 times) Fe level in Zy, but not in ZN2: it is not clear why this difference in behaviour exists. It is also apparent that the highest Fe alloy, ZN4, has the highest pre- and post-irradiation Fe levels. This may be associated with the presence of intra-granular second-phase particles, suggested from microscopic observations [15].

Exp. 3. The results show that the Fe levels in the IRV increase with the Fe concentrations of the alloys for both 20 and 10 kV SEM operating voltages. At 420°C, the Fe concentrations are much higher than the corresponding 303°C values. At 10 kV, Fe levels are almost double those at 20 kV, as in Ref. [7], this shows higher pseudo-equilibrium Fe levels (see below) nearer the surface of the IRV. Since the average Fe levels in the IRV exceed the overall alloy Fe concentrations Fe must have migrated into the IRV from below — see also Ref. [7]: this is supported by the present data for Ar irradiated Zr(Fe) single crystals, see below.

Exp. 4. In comparison with Exp. 3 the irradiation dose/time has been doubled. There is no apparent increase in the Fe levels in the α-grains; the result from a thin foil specimen is similar. This suggests that a four hour, 2×10^{20} m^{-2} exposure at 420°C is sufficient to create pseudo-equilibrium conditions.

Exp. 5. Here ZN3 was irradiated at a higher temperature for a longer time, but again the measured IRV Fe level is similar to those found for Exps. 3 and 4.

Exp. 6. The data here are for the highest irradiation temperature and a relatively short time. Again there is an indication of relative, near-saturation Fe levels, c.f. exps. 3–5: the exceptional ZN4 result, in this context, may be indicative of an upper-level, temperature-effected, steady-state Fe level under irradiation.

Exp. 7. The results here are generally similar to those from Exp. 3. This suggests that the population of freely

migrating defects (FMD), vacancies and self-interstitials, for both irradiations are similar.

Exp. 8. The short irradiation time gives a measure of the kinetics of Fe dissolution. All the Fe levels are much lower that those from Exps. 3 and 4. The relatively high Fe level of ZN3 could reflect a grain-size effect. For similar grain sizes, ZN2 and ZN4, the Fe level of ZN4 is always higher, probably a result of the higher driving force (Fe concentration) causing Fe to flow from the β- to the α-phase.

Exp. 9. This low-flux/low fluence experiment shows only marginal increases in the α-phase Fe levels of the IRV. It is probable, in view of the near-saturation Fe levels suggested by Exps. 3–6, that we are seeing a flux effect here. The flux (damage rate) is likely the predominant factor governing the pseudo-steady-state vacancy concentration, which, in turn, affects the Fe concentration through the formation of a meta-stable Fe-vacancy complex [16].

Exp. 10. Trim calculations [14] show that the 1.5 MeV Kr damage profile is slightly shallower than the equivalent (energy) Ar one and that its damage rate is double that of Ar. However, for a similar dpa rate (half of the flux for Exp. 3) the α-phase Fe levels tend to be much lower than those in Exp. 3. This may reflect a lower FMD production rate.

In Table 2, the EDX measurements of the Fe levels in the β-phase of irradiated foils show that the Fe levels have decreased from about 1.5% to 0.4%. These results are in qualitative agreement with those of the previous studies [5,6].

3.3. Zr single crystal

A basal-plane-surfaced α-Zr single crystal specimen was irradiated with 1.5 MeV Ar^+ at 419°C for 5.2 h to a fluence of 1.96×10^{20} m^{-2}.

The Fe concentration/depth profiles of the reference-state (RSX) and irradiated (ISX) single crystals are shown in Fig. 2. There are the usual, high near-surface segregated Fe levels for both specimens [17] followed by notably different distributions in the bulk.

The 'surface' Fe concentration for the RSX is about three orders of magnitude higher than the bulk level, which is reached at a depth of ~ 300 nm. In sharp contrast, the surface Fe level of the ISX is only about ten times higher than that of the bulk; at ~ 300 nm there is a plateau (~ 1.2 μm wide) with an Fe concentration that is about five times the bulk level. There is then a 'trough' in the Fe concentration before it returns slowly towards its original bulk level. The boundary at 1.2 μm corresponds quite well to the depth of the IRV; the shape of the Fe distribution beyond there is associated with transport of Fe from the bulk to its enhanced level in the IRV.

The lower surface Fe concentration of the ISX is associated with the irradiation-driven depletion of the Fe-rich surface segregation layer expected from the 420°C

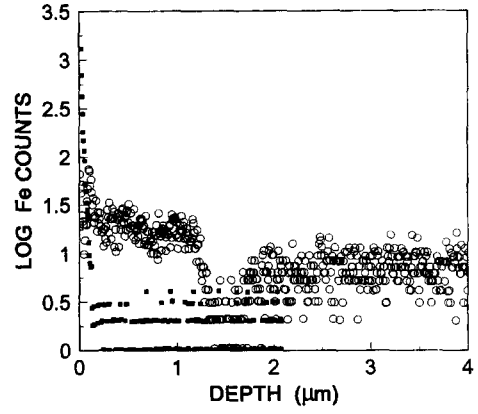

Fig. 2. SIMS profiles of Fe distributions in α-Zr single crystals $< 0001 >$, ■, unirradiated; and ○, irradiated with 1.5 MeV Ar^+ for 5.2 h at 419°C to 1.96×10^{20} m^{-2}.

heating treatment [17]. The high plateau Fe levels of the IRV of the ISX, coupled with the rest of the depth profile, show that Fe has migrated into the IRV, not only from the surface but also from the bulk. Extrapolation of Fe tracer diffusion data [18] for α-Zr single crystals leads to a diffusion coefficient, $D_{\|} \sim 10^{-14}$ m^2/s at 420°C, where $D_{\|}$ refers to diffusion parallel to the *c*-axis. In the present context the expected mean bulk diffusion distance for Fe is, $(Dt)^{0.5} \sim 14$ μm, this is sufficient to account for the observed Fe build-up.

3.4. Phenomenology

Fig. 3 shows how the Fe redistribution in ZN may take place during Ar irradiation. A similar picture is expected for Zy, replacing the β-phase with grain boundary precipitates. The ability of Fe to transfer from the unirradiated to the irradiated α-phase volume is graphically illustrated by the results for the single-crystal experiment. This transport

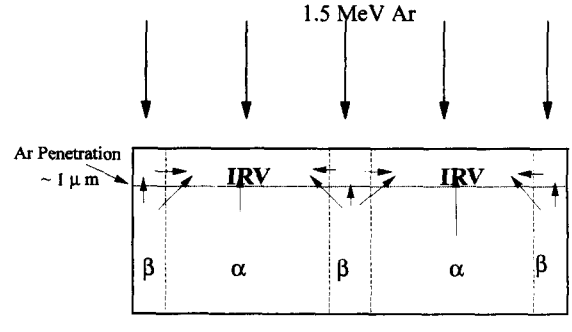

Fig. 3. Postulated Fe movements in polycrystalline Zr alloys during irradiation. The designation 'IRV' means the irradiated volume of the specimen.

process can evidently lead to irradiation-driven maximum Fe levels in the irradiated α-phase which are in excess of the overall Fe concentrations in the alloys.

A driving force is needed to cause Fe atoms to diffuse into the α-phase against the thermal equilibrium state (from below to the IRV for Zr single crystal). It is possible that the irradiation-driven increase in Fe concentration is related to the excess vacancy concentration and the resultant formation of very strongly bound Fe-vacancy complexes [16]. After the system reaches a pseudo-steady state there will be a corresponding vacancy flux toward sinks, mostly dislocations generated by the irradiation. When vacancies annihilate at dislocations, Fe atoms are left to segregate at the dislocations. This has been observed in electron-irradiated Ti [19].

4. Concluding remarks

This work has shown that energetic particle irradiation (mostly 1.5 MeV Ar^+) of Zr–2.5Nb (with four different Fe concentrations), Zircaloy-2 and nominally pure Zr single crystals can lead to remarkable enhancement of the α-phase Fe levels in the irradiated volumes (IRV). The Fe concentrations may be as high as one thousand times the thermal equilibrium α-phase TSS limits. Effects of irradiation temperature, specimen composition (Fe level), irradiating particle and irradiation flux and dose have been studied: in addition, some Fe levels in the IRV were examined at two depths. The principal results seem to be as follows.

(1) Temperature: The results for Zr–2.5Nb show a limited IRV increase in Fe from 50–300°C, a large increase between 300 and 420°C and then little further temperature effect up to 480°C. The Zircaloy-2 results show strong IRV α-phase enhancement at 300°C. The single-crystal experiment, done at 420°C, shows strongly enhanced IRV Fe concentrations, showing that Fe diffusion transfer from the bulk of the crystal has occurred.

(2) Composition: For a given irradiation, the IRV enhancement of the Fe levels (Zr–2.5Nb) shows an almost proportionate increase with the alloy Fe concentration.

(3) Depth: Without exception, the IRV Fe levels measured with a 10 kV, vis a vis 20 kV, electron probing beam are higher.

Acknowledgements

The authors are grateful to Dawson Phillips and Doug Bonnett for assistance with the irradiations. Funding for this work came from the Candu Owners Group, Working Party 32.

References

[1] M. Griffiths, R.W. Gilbert and G.J.C. Carpernter, J. Nucl. Mater. 150 (1987) 53.
[2] M. Griffiths, J. Nucl. Mater. 159 (1988) 190.
[3] Y. Etoh and S. Shimada, J. Nucl. Mater. 200 (1993) 59.
[4] A.T. Motta and C.A. Lemaignan, J. Nucl. Mater. 195 (1992) 277.
[5] M. Griffiths, P.C.K. Chow, C.E. Coleman, R.A. Holt, S. Sagat and V.F. Urbanic, Effects of Radiation on Materials, 16th Int. Symp., Aurora, 23–25 June (1992), STP1175, pp. 1077–1110.
[6] V. Perovic, A. Perovic, G.C. Weatherly and G.R. Purdy, J. Nucl. Mater. 224 (1995) 93.
[7] H. Zou, G.M. Hood, J.A. Roy and R.H. Packwood, Mater. Res. Soc. Symp. Proc. 373 (1995) 201.
[8] H. Zou, G.M. Hood, J.A. Roy, R.J. Schultz and J.A. Jackman, J. Nucl. Mater. 210 (1994) 239.
[9] G.M. Hood, Defect Diffus. Forum 95–98 (1994) 755.
[10] T. Laursen, G.M. Hood, R. Belec, G.R. Palmer, R.J. Schultz and J.L. Whitton, Nucl. Instrum. Methods B64 (1992) 475.
[11] M. Griffiths, R.W. Gilbert and V. Fidleris, ASTM-STP 1023 (1989) 658.
[12] R.G. Fleck, J.E. Elder, A.R. Causey and R.A. Holt, in: Zirconium in the Nuclear Industry, Ninth Int. Symp., ASTM STP 1245 (1995) p. 168.
[13] H. Zou, G.M. Hood, J.A. Roy, R.H. Packwood and V. Weatherall, J. Nucl. Mater. 208 (1994) 159.
[14] J.P. Biersack and U. Littmark, The Stopping and Range of Ions in Solids by J.F. Ziegler (Pergamon, New York, 1985), update version 92.19.
[15] J. NG-Yelim, O.T. Woo and G.J.C. Carpenter, J. Elec. Microsc. Tech. 15 (1990) 400.
[16] A.D. King, G.M. Hood and R.A. Holt, J. Nucl. Mater 185 (1991) 174.
[17] C-S. Zhang, B. Li and P.R. Norton, J. Nucl. Mater. 223 (1995) 238.
[18] H. Nakajima, G.M. Hood and R.J. Schultz, Philos. Mag. B58 (1988) 319.
[19] M. Griffiths, J. White, M.H. Loretto and R.E. Smallman, in: Metals, eds. J. Takamura, M. Doyama and M. Kiritani (University of Tokyo, 1982) p. 879.